KYBERNETIKA — VOLUME *54* (2018), NUMBER 6, PAGES 1184–1200

MULTISTAGE MULTIVARIATE NESTED DISTANCE: AN EMPIRICAL ANALYSIS

Sebastiano Vitali

Multistage stochastic optimization requires the definition and the generation of a discrete stochastic tree that represents the evolution of the uncertain parameters in time and space. The dimension of the tree is the result of a trade-off between the adaptability to the original probability distribution and the computational tractability. Moreover, the discrete approximation of a continuous random variable is not unique. The concept of the best discrete approximation has been widely explored and many enhancements to adjust and fix a stochastic tree in order to represent as well as possible the real distribution have been proposed. Yet, often, the same generation algorithm can produce multiple trees to represent the random variable. Therefore, the recent literature investigates the concept of distance between trees which are candidate to be adopted as stochastic framework for the multistage model optimization. The contribution of this paper is to compute the nested distance between a large set of multistage and multivariate trees and, for a sample of basic financial problems, to empirically show the positive relation between the tree distance and the distance of the corresponding optimal solutions, and between the tree distance and the optimal objective values. Moreover, we compute a lower bound for the Lipschitz constant that bounds the optimal value distance.

Keywords: multistage stochastic optimization, nested distance, portfolio models

Classification: 90C15, 60B05, 62P05

1. INTRODUCTION

Real world is complex and highly structured. Several approaches have been proposed to solve decision problems under uncertainty. One of the most promising is stochastic optimization that addresses the issue of finding an optimal solution today in order to reduce the cost to adjust the solution after the realization of an uncertain event in the future, see [1] and [15]. When the stochastic random variable and the optimal decision evolve along a sequence of temporal stages, the framework becomes a multistage stochastic optimization, see [17]. Financial problems require models that very well interface with multistage stochastic optimization because they typically need to find an optimal portfolio allocation in financial assets whose future return is uncertain, see [2, 3, 5, 6, 19]. Therefore, the implementation of a multistage stochastic model follows the characterization of the stochastic environment in which the problem is defined. Such environment

DOI: 10.14736/kyb-2018-6-1184

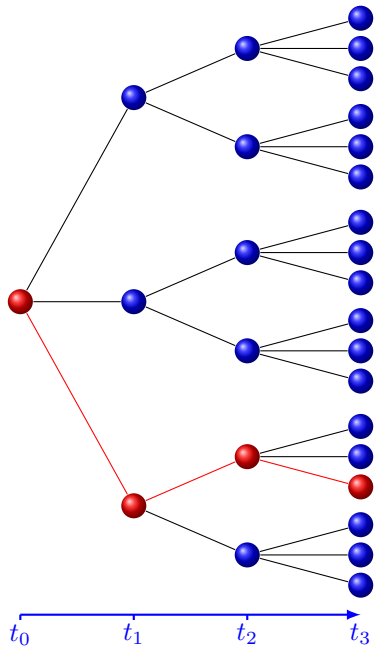

Fig. 1. Example of stochastic tree evolving on three stages and having branching 3-2-3.

consists in random parameters which are described by continuous distributions. For computational reasons, the continuous distribution must be approximated with a discrete representation that takes the name of stochastic tree. Figure 1 shows an example of discrete multistage stochastic tree having a regular branching which means that each node has the same number of children as the other nodes in the same stage. In particular, in the example the root node has three children, each of them has two children and each of these has three children. We denote such type of branching as 3-2-3. Each path that connects the root node with one of the node of the last stage is called scenario. The tree in Figure 1 is composed of 18 scenarios.

Discrete stochastic trees generated under the same distributional assumptions can be very different and therefore may produce different optimal objective values and different solutions, see [8, 9] and [10] for different methods to obtain lower and upper bounds based on finite scenario tree approximations. The purpose of this paper is to investigate if there exists a concrete and empirical relation between the level of similarity of the tree and the distance between the optimal objective values and the optimal solutions. We highlight that such relation differs according to the implemented objective function. To compute the similarity between the trees we adopt the nested distance proposed in [11] and [12] and we empirically show that the Lipschitz constant theorized in [11] which bounds the optimal objective distances represents a weak constraint in the sense that most of the solutions are relatively far from the bound. The paper is structured as

follows. In Section 2 we introduce three basic multistage portfolio selection models that will be used in the further analysis. In Section 3 we recall the nested distance algorithm and its extension for the case of multivariate multistage stochastic tree. Then, in Section 4 we propose a selection of stochastic trees based on different generation assumptions and in Section 5 we conduct an empirical analysis of the relation between nested distance, optimal solution distance and optimal objective function distance. Section 7 summarizes the results and propose future research extensions.

2. PORTFOLIO SELECTION MODELS

To produce results about the sensitivity of the solution distance with respect to the tree distance, we propose three portfolio models very well known in the literature that discusses stochastic optimization applied to financial problems, see e. g. [2, 5, 6, 19]. The three models are: the maximization of the average value-at-risk (AV@R), the maximization of the expected wealth and the minimization of the difference between the expected wealth and its AV@R. In particular, the third model has recently been studied in [6] and [4].

Given a set $i = 1, \dots, N$ of assets, a sequence of stages $t_k = t_0, \dots, T$ and a set of scenarios $s = 1, \dots, S$ having each probability p_s, we can define the variables of the optimization problem:

$x^+_{i,t_k,s}$ $x^-_{i,t_k,s}$ represent, respectively, how much we buy and how much we sell of asset i at stage t_k on scenario s,

$h_{i,t_k,s}$ represents the holding in asset i at stage t_k on scenario s,

$w_{t_k,s}$ represents the total wealth of the portfolio at stage t_k on scenario s,

z_s is the slack variable for the AV@R formulation as proposed in [16].

The random variable is the rate of return $\rho_{i,t_k,s}$ that expresses the growing rate of asset i realized in stage t_k from stage t_{k-1} on scenario s. Other parameters are: the confidence level α for the AV@R definition, the initial wealth w_0, and the turnover coefficient θ.

$$\max \quad \beta_1 \cdot \left(\sum_{s=1}^{S} (w_{T,s} \cdot p_s) \right) + \beta_2 \cdot \left(a - \frac{1}{\alpha} \sum_{s=1}^{S} (z_s \cdot p_s) \right) \tag{1}$$

$$\text{s.t.} \quad -a + w_{T,s} + z_s \geq 0, \quad z_s \geq 0, \ \ \forall s \tag{2}$$

$$\sum_{i=1}^{N} x^+_{i,t_0,s} = w_0, \ \ \forall s \tag{3}$$

$$h_{i,t_0,s} = x^+_{i,t_0,s}, \ \ \forall i, \forall s \tag{4}$$

$$h_{i,t_k,s} = h_{i,t_{k-1},s} \cdot (1 + \rho_{i,t_k,s}) + x^+_{i,t_k,s} - x^-_{i,t_k,s}, \ \ \forall i, t_0 < t_k \leq T, \forall s \tag{5}$$

$$w_{t_k,s} = \sum_{i=1}^{N} h_{i,t_k,s}, \ \ \forall t_k, \forall s \tag{6}$$

$$\sum_{i=1}^{N} x^+_{i,t_k,s} = \sum_{i=1}^{N} x^-_{i,t_k,s}, \ \ t_0 < t_k \leq T, \forall s \tag{7}$$

$$x^{-}_{i,t_k,s} \leq h_{i,t_{k-1},s} \cdot (1 + \rho_{i,t_k,s}), \quad \forall i, t_0 < t_k \leq T, \forall s \tag{8}$$

$$\sum_{i=1}^{N} x^{-}_{i,t_k,s} \leq \theta \cdot w_{t_k,s}, \quad t_k \leq T, \forall s \tag{9}$$

$$x^{+}_{i,t_k,s} \geq 0, \quad x^{-}_{i,t_k,s} \geq 0, \quad , \quad \forall i, \forall t_k, \forall s. \tag{10}$$

Moreover, since we use a stochastic tree structure, we include the set of all the non-anticipativity constraints on the decision variables. The three proposed models are obtained by imposing respectively:

- $\beta_1 = 0$ and $\beta_2 = 1$: AV@R maximization,
- $\beta_1 = 1$ and $\beta_2 = 0$: expected wealth maximization,
- $\beta_1 = -1$ and $\beta_2 = 1$: expected wealth – AV@R minimization.

3. MULTISTAGE MULTIVARIATE NESTED DISTANCE FORMULATION

The nested distance between two multistage tree has been proposed in [11] and [12]. Further, it has been investigated in other papers, see e. g. [13, 18], and it has been adopted also as approach for the stochastic tree generation, see [14] and [7]. The nested distance proposed in [11] and [12] is consistent with different distance measures. In this paper we use the Wasserstein distance as adopted in [12][1]. Moreover, we need to extend the proposed algorithm which is constructed for a univariate multistage tree to a multivariate multistage tree since, instead of having only one random variable in each node, we have the random vector of the asset returns. Then, let's assume that we want to compute the nested distance between stochastic tree $\mathcal{T}$ composed of nodes n_{s,t_k} (nodes on scenario s and at stage t_k) and stochastic tree $\tilde{\mathcal{T}}$ composed of nodes $n_{\tilde{s},t_k}$ (nodes on scenario $\tilde{s}$ and at stage t_k). The nodal distance $d(n_{s,t_k}, n_{\tilde{s},t_k})$ between node n_{s,t_k} and node $n_{\tilde{s},t_k}$ cannot be computed as $d(n_{s,t_k}, n_{\tilde{s},t_k}) = |\xi_{s,t_k} - \xi_{\tilde{s},t_k}|$ as in the case of univariate stochastic variable ξ, but it can be computed as $d(n_{s,t_k}, n_{\tilde{s},t_k}) = \left\|\bar{\xi}_{s,t_k} - \bar{\xi}_{\tilde{s},t_k}\right\|_1$ where $\bar{\xi}$ is the multivariate stochastic vector of node n_{s,t_k}. In the model proposed in Section 2, the nodal vector $\bar{\xi}_{s,t_k}$ is the vector composed of the returns of all the assets $\rho_{i,t_k,s}$ in stage t_k and scenario s. Then, the distance $d(s_i, \tilde{s}_j)$ between scenario s_i and scenario $\tilde{s}_j$ is computed as $d(s_i, \tilde{s}_j) = \sum_{t_k=t_0}^{T} d(n_{s_i,t_k}, n_{\tilde{s}_j,t_k})$. Once the distances between each couple of scenarios are computed, we proceed backward as suggested by the algorithm in [12] to define the *tree distance* $d(\mathcal{T}, \tilde{\mathcal{T}})$ between trees $\mathcal{T}$ and $\tilde{\mathcal{T}}$.

4. SCENARIO GENERATION

To produce a wide sensitivity analysis of the relation between the tree distances and the solution distances, we create different sets of trees. As database, we consider the historical series composed by 500 monthly returns of 10 financial indexes with a wide variety of risk/return profiles. A first approach to generate the scenarios moves from the estimation of the historical average and volatility of the returns. Then, we generate

[1] see Algorithm 2.1 in [12], p. 86.

– with a Monte Carlo approach – the asset returns for each node of the tree under a geometric Brownian motion (GBM) assumption. The asset returns of each node are hereafter referred to as nodal coefficients. The Monte Carlo procedure is repeated for each node of the tree to construct a multistage multivariate stochastic tree that evolves from an initial time t_0 along 4 stages, i. e. $t = t_0, t_1, t_2, t_3, t_4$, and has a regular branching 5-5-2-2, i. e. 100 scenarios. According to the formulation of model (1)–(10), the return in t_0 is not relevant and then it is always set to zero. Such procedure is repeated to generate a set of 100 trees which will be denoted as $\mathcal{T}_{GBM,0} = \{\mathcal{T}^p_{GBM,0},\ p = 1, \ldots, 100\}$. Then, we use again the Monte Carlo procedure to generate the set $\mathcal{T}_{GBM,1} = \{\mathcal{T}^p_{GBM,1},\ p = 1, \ldots, 100\}$ whose trees have in common the nodal coefficients of the first stage t_1 and differ from each other due to the nodal coefficients in stages t_2, t_3, t_4. Similarly, we repeat the procedure to generate 100 trees which have in common the nodal coefficients of the first two stages and we obtain the set $\mathcal{T}_{GBM,2} = \{\mathcal{T}^p_{GBM,2},\ p = 1, \ldots, 100\}$. Finally, we generate the set $\mathcal{T}_{GBM,3} = \{\mathcal{T}^p_{GBM,3},\ p = 1, \ldots, 100\}$ of trees that have in common the nodal coefficients of the first three stages and differ due to the last stage nodal coefficients. To summarize:

1. $n_{t_k,s} \in \mathcal{T}^p_{GBM,0}, \tilde{n}_{t_k,s} \in \mathcal{T}^q_{GBM,0}, p \neq q \Rightarrow n_{t_k,s} \neq \tilde{n}_{t_k,s} \forall t_k$
2. $n_{t_k,s} \in \mathcal{T}^p_{GBM,1}, \tilde{n}_{t_k,s} \in \mathcal{T}^q_{GBM,1}, p \neq q \Rightarrow n_{t_k,s} \neq \tilde{n}_{t_k,s},\ t_k = t_2, t_3, t_4,\ n_{t_k,s} = \tilde{n}_{t_k,s},\ t_k = t_1$
3. $n_{t_k,s} \in \mathcal{T}^p_{GBM,2}, \tilde{n}_{t_k,s} \in \mathcal{T}^q_{GBM,2}, p \neq q \Rightarrow n_{t_k,s} \neq \tilde{n}_{t_k,s},\ t_k = t_3, t_4,\ n_{t_k,s} = \tilde{n}_{t_k,s},\ t_k = t_1, t_2$
4. $n_{t_k,s} \in \mathcal{T}^p_{GBM,3}, \tilde{n}_{t_k,s} \in \mathcal{T}^q_{GBM,3}, p \neq q \Rightarrow n_{t_k,s} \neq \tilde{n}_{t_k,s},\ t_k = t_4,\ n_{t_k,s} = \tilde{n}_{t_k,s},\ t_k = t_1, t_2, t_3$

To compare with an alternative scenario generation procedure, we adopt the historical extraction proposed in [6] which requires neither any estimation nor any distribution assumption on the returns and generates the trees thanks to a pseudo-random extraction from the historical series. Such generation is able to keep the asset correlations, it maintains the economic cycles and produces a wide representation in terms of "good" and "bad" scenarios even in case of small branching. We run the algorithm 100 times to obtain another set of trees denoted $\mathcal{T}_{HIST} = \{\mathcal{T}^p_{HIST},\ p = 1, \ldots, 100\}$.

5. EMPIRICAL RESULTS

In this section, we discuss the results obtained by solving the portfolio selection model (1) – (10) and fixing the model parameters: α =5%, w_0 =100, θ =80% and, according to the scenario generation procedure just described, $p_s = 1/S$, i. e. the scenarios are equiprobable. In particular, considering the three portfolio models and the five tree sets, we investigate whether to an increasing tree distance corresponds an increasing objective distance and an increasing solution distance. Therefore, we solve each portfolio selection model for all trees of each tree set.

Denoting $O_{\mathcal{T}^p}$ the objective optimal value obtained with the tree $\mathcal{T}^p$, the *objective distance* is defined as

$$d(O_{\mathcal{T}^p}, O_{\mathcal{T}^q}) = |O_{\mathcal{T}^p} - O_{\mathcal{T}^q}| \tag{11}$$

while, denoting $\mathbf{h}^{\mathcal{T}^p}_{t_0,s} = [h^{\mathcal{T}^p}_{1,t_0,s}, \ldots, h^{\mathcal{T}^p}_{N,t_0,s}]^\top$ the vector of the optimal portfolio allocation in the root node – hereafter referred to as the here-and-now (H&N) allocation – obtained with the tree $\mathcal{T}^p$, the *solution distance* is computed as

$$d(\mathbf{h}^{\mathcal{T}^p}_{t_0,s}, \mathbf{h}^{\mathcal{T}^q}_{t_0,s}) = \frac{1}{2}||\mathbf{h}^{\mathcal{T}^p}_{t_0,s} - \mathbf{h}^{\mathcal{T}^q}_{t_0,s}||_1 \tag{12}$$

where for $\mathbf{x} = [x_1, \ldots, x_N]^\top$, $||\mathbf{x}||_1 = \sum_{i=1}^N |x_i|$. A solution distance equal to 1 corresponds to two H&N portfolio allocations completely different from each other.

Finally, for each couple of trees of each tree set, we compute the tree distance, the objective distance and the solution distance, and provide empirical evidences of the relation between these distances.

In all the Figures of the current section, to a different tree set corresponds a different color[2] according to the following legend:

$\mathcal{T}_{GBM,0}$**:** purple asterisk

$\mathcal{T}_{GBM,1}$**:** yellow asterisk

$\mathcal{T}_{GBM,2}$**:** red asterisk

$\mathcal{T}_{GBM,3}$**:** blue asterisk

$\mathcal{T}_{HIST}$**:** green dot

All the results have been computed with an algorithm coded and performed in MATLAB R2013b, with an Intel(R) Core(TM) i7-4510U CPU 2.60GHz with 8.00GB RAM running Windows 10. The portfolio models are fully linear programming problems. Moreover, because of the purpose of the current work and to produce a large comparison, each single tree dimension is relatively small and then the solver CPLEX 12.1 takes few seconds to find the optimal solution. To compute the distance between each couple of trees the algorithm takes approximately 20 seconds.

5.1. AV@R portfolio model

The first analysis is conducted using the AV@R maximization model. Figure 2 reports the relation between the tree distances and the objective distances. As expected, the different tree sets produce tree distances that span in disjoint ranges, while the trees in the same set have a substantially homogeneous distance. Therefore, the points turn out to be naturally clustered according to the tree set. The only exception is represented by the $\mathcal{T}_{HIST}$ set that overlaps with both the $\mathcal{T}_{GBM,0}$ and the $\mathcal{T}_{GBM,1}$. In particular, the average values of the tree distance are 0.51 for $\mathcal{T}_{GBM,3}$, 1.00 for $\mathcal{T}_{GBM,2}$, 1.37 for $\mathcal{T}_{GBM,1}$, 1.76 for $\mathcal{T}_{GBM,0}$ and 1.68 for $\mathcal{T}_{HIST}$. Moving from a tree set to a tree set with larger average tree distance, the cloud of points becomes more sparse and the objective distance increases showing a positive relation between the two quantities. The box-plot representation highlights further the increasing objective distance averages which are

[2] For colored figures please see an electronic version:
https://www.kybernetika.cz/content/2018/6/1184

1.77 for $\mathcal{T}_{GBM,3}$, 2.29 for $\mathcal{T}_{GBM,2}$, 2.65 for $\mathcal{T}_{GBM,1}$, 3.16 for $\mathcal{T}_{GBM,0}$ and 3.94 for $\mathcal{T}_{HIST}$. We report in Table 1 a complete description of the distance statistics. In particular, for $\mathcal{T}_{HIST}$, we observe a smaller tree distance than $\mathcal{T}_{GBM,0}$, considering that both the tree sets are generated with a fully random approach, i. e. not fixing the nodal values as in the other cases. This behavior suggest that the historical scenario generation technique represents the information in a more homogeneous way than a fully random generation.

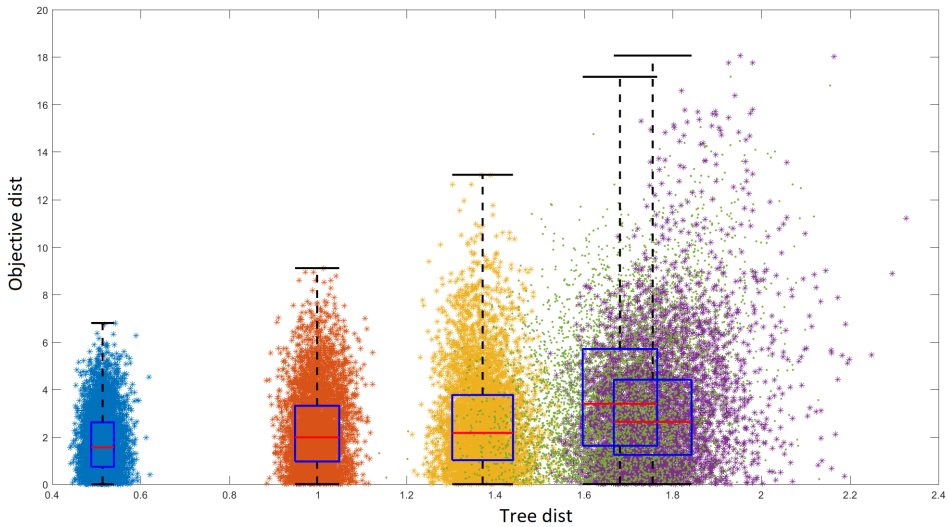

Fig. 2. Objective distance in relation with the tree distance for the AV@R maximization model and corresponding box-plot for each tree set.

In Figure 3 we observe the relation between the tree distances and the solution distances. For all sets, the figure highlights an increasing solution distance average for increasing tree distance average. In particular, the solution distance averages are 0.28 for $\mathcal{T}_{GBM,3}$, 0.47 for $\mathcal{T}_{GBM,2}$, 0.56 for $\mathcal{T}_{GBM,1}$, 0.80 for $\mathcal{T}_{GBM,0}$ and 0.81 for $\mathcal{T}_{HIST}$. For set $\mathcal{T}_{GBM,3}$ only very few couples of trees propose a completely different H&N allocation, while in the $\mathcal{T}_{GBM,0}$ case most of the solution distances are close to 1 which is the maximum value reachable according to formula 12. This means that a relatively small tree distance ensures a stability of the optimal allocation in the root node.

Figure 4 shows the relation between the objective distance and the solution distance. The clouds of the points of the different tree sets are not distinct from each other as in the previous figures. In general, we do not observe an increasing objective distance for increasing solution distance. This means that a small solution distance does not correspond necessarily to a small objective distance and vice versa. Figure 5 presents the relations between the three analyzed distances for the AV@R case. We observe a sort of cone departing from the origin that highlight the joint increasing movements on

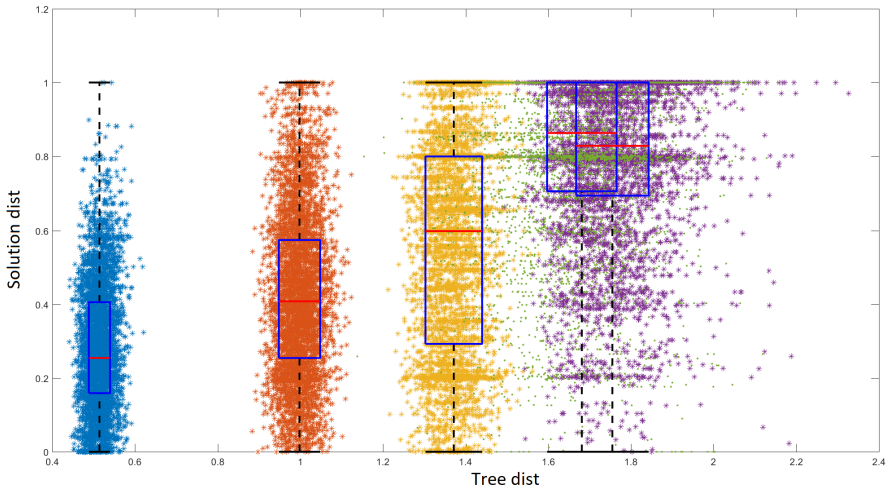

Fig. 3. Solution distance in relation with the tree distance for the AV@R maximization model and corresponding box-plot for each tree set.

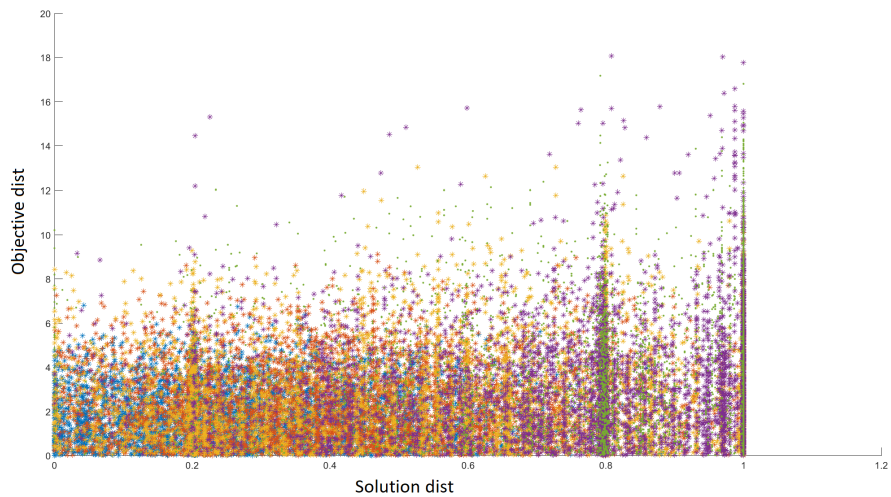

Fig. 4. Objective distance in relation with the solution distance for the AV@R maximization model.

the three dimensions. However, also from this perspective, the solution distance seems not to influence the objective distance remarkably.

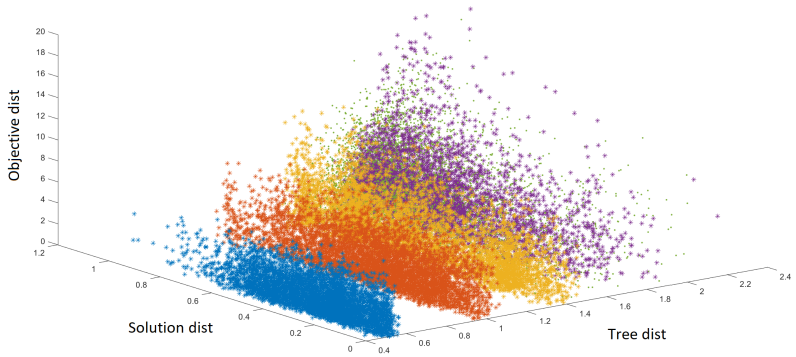

Fig. 5. Relation between objective distance, solution distance and tree distance for the AV@R maximization model.

5.2. Expected value portfolio model

The second portfolio model that we investigate is the expected wealth maximization. In Figure 6 we show the relation between the tree distance and the objective distance. With respect to the AV@R case, the objective distance averages increase more evidently with the tree distance averages. The objective distance averages are 0.60 for $\mathcal{T}_{GBM,3}$, 1.09 for $\mathcal{T}_{GBM,2}$, 1.45 for $\mathcal{T}_{GBM,1}$, 3.00 for $\mathcal{T}_{GBM,0}$ and 2.88 for $\mathcal{T}_{HIST}$. The box-plot analysis strengthens this evidence both in terms of objective distance averages and in terms of objective distance volatilities. In particular, both the $\mathcal{T}_{HIST}$ and $\mathcal{T}_{GBM,0}$ clouds of points are much more sparse than the other sets and have some couples of trees with remarkably high objective distance. In Figure 7 we report the solution distances. For the cases $\mathcal{T}_{GBM,3}$ and $\mathcal{T}_{GBM,2}$, almost all the solution distances are zero underlying a very similar allocation determined by the nodal coefficients of the first stages which are common between the different trees. Moving to $\mathcal{T}_{GBM,1}$ we observe mainly three different H&N allocations and, therefore, the solution distances are concentrated around 0, 0.2 and 0.4. The cases $\mathcal{T}_{HIST}$ and $\mathcal{T}_{GBM,0}$ also show four main groups of solution distances (0, 0.2, 0.8 and 1) corresponding to four representative H&N allocations. This represents a relevant difference in comparison with the AV@R maximization model for which we obtained much more diversified H&N allocations. Therefore, the small diversification of the H&N portfolio induced by the model is reflected by the objective distance measure. Figure 8 presents the relation between solution distance and objective distance. As observed in Figure 7, the solution distances are highly concentrated on a restricted set of points. The $\mathcal{T}_{GBM,1}$, $\mathcal{T}_{GBM,2}$ and $\mathcal{T}_{GBM,3}$ are concentrated in the low-left side of the graph, while the $\mathcal{T}_{GBM,0}$ case is much more sparse and the $\mathcal{T}_{HIST}$ is concentrated in the top-right side. Therefore, in this case, very high values of objective distance are reached only in correspondence of very different H&N allocations. Such observation is confirmed by Figure 8 in which it is clear that the three distances increase together.

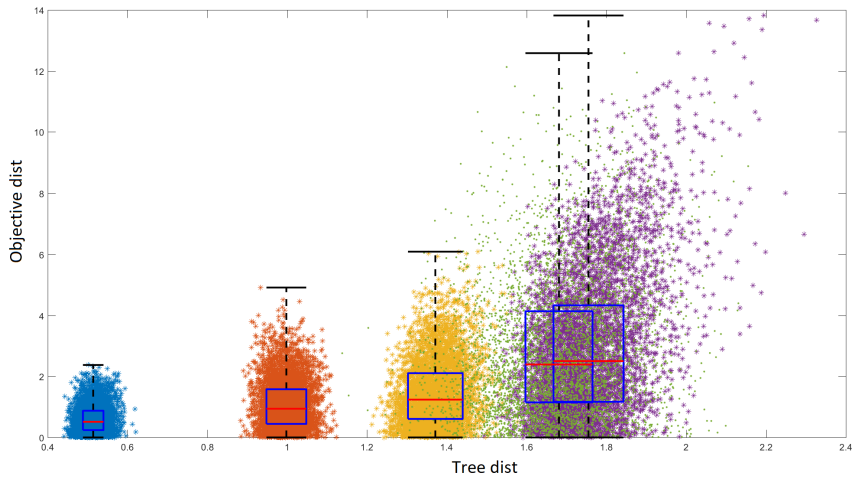

Fig. 6. Objective distance in relation with the tree distance for the expected wealth maximization model and corresponding box-plot for each tree set.

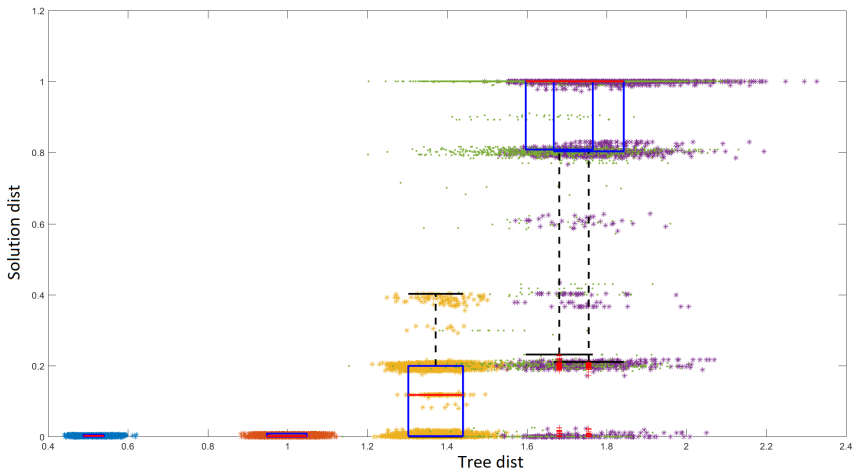

Fig. 7. Objective distance in relation with the tree distance for the expected wealth maximization model and corresponding box-plot for each tree set.

In particular, all the distances of sets $\mathcal{T}_{GBM,3}$ and $\mathcal{T}_{GBM,2}$ are quite small, set $\mathcal{T}_{GBM,1}$ presents medium distances, while the distances of sets $\mathcal{T}_{GBM,0}$ and $\mathcal{T}_{HIST}$ are sparse and reach high values.

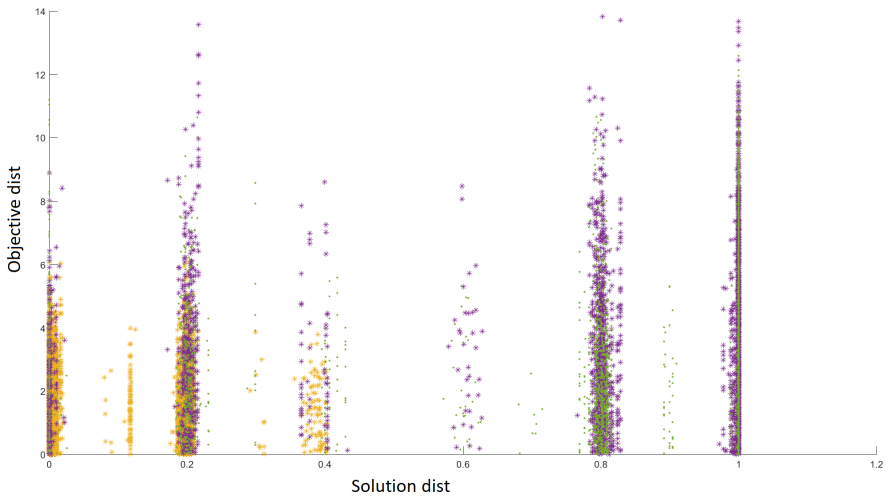

Fig. 8. Objective distance in relation with the solution distance for the expected wealth maximization model.

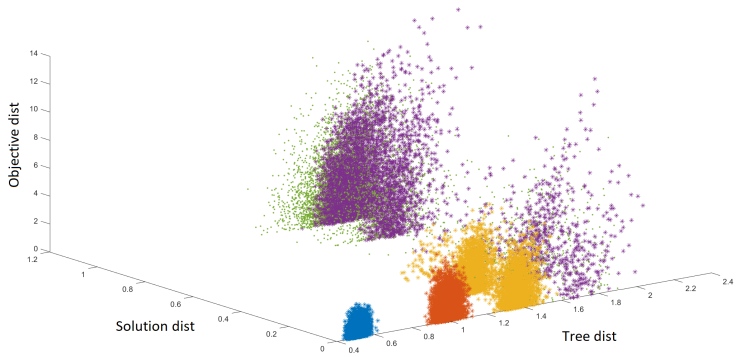

Fig. 9. Relation between objective distance, solution distance and tree distance for the expected wealth maximization model.

5.3. Expected value – AV@R portfolio model

The last portfolio model that we study is based on the minimization of the difference between the expected value and the AV@R of the final wealth. In Figure 10 we report the relation between the tree distances and the optimal objective distances. In this case, the evidence that a larger tree distance corresponds to a larger objective value distance is less strong than in the previous cases. The objective distance averages are 0.95 for $\mathcal{T}_{GBM,3}$,

0.75 for $\mathcal{T}_{GBM,2}$, 1.00 for $\mathcal{T}_{GBM,1}$, 0.94 for $\mathcal{T}_{GBM,0}$ and 1.53 for $\mathcal{T}_{HIST}$. Therefore, increasing tree distance averages of the different tree sets are not followed by increasing objective distance averages and to observe a comovement between the objective distance and the tree distance is necessary to resort to other statistics: comparing the maximum distance and the standard deviation we observe that both increase as the tree distance average increases, see Table 1. Such result could be explained by the type of objective function considered. For instance, considering two different trees, it can happen that the averages of the wealths on the two trees are very far from each other as well as the AV@Rs of the wealth distributions, still the respective differences turn out to be very close. However, we consider important to remark that it makes sense to compare and interpret the distances considering the peculiarities of the objective function not only from a mathematical point of view, but also from a financial point of view.

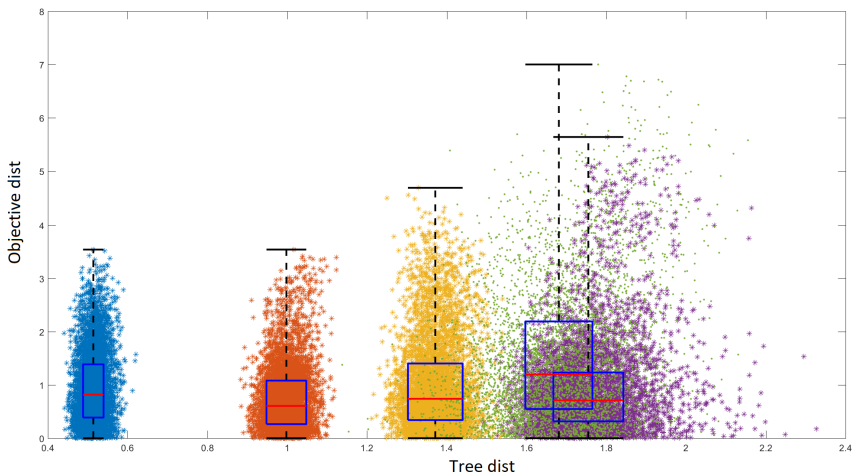

Fig. 10. Objective distance in relation with the tree distance for the expected wealth – AV@R minimization model and corresponding box-plot for each tree set.

As confirmation of the previous comment, the anomaly highlighted in the case of objective distance partially disappears in Figure 11 where we consider the solution distance. Indeed, the solution distance averages are 0.27 for $\mathcal{T}_{GBM,3}$, 0.46 for $\mathcal{T}_{GBM,2}$, 0.60 for $\mathcal{T}_{GBM,1}$, 0.75 for $\mathcal{T}_{GBM,0}$ and 0.78 for $\mathcal{T}_{HIST}$. As in the AV@R model case, the solutions are quite diversified from each other and do not polarize on a small set of H&N allocations. Figure 12 presents the relation between the objective distance and the solution distance. Here, the distribution of colors, compared to Figure 4, gives a clearer vision of the position occupied by the different tree sets, even if still overlapping. However, the objective distance does not seem to increase as the solution distance increases. Figure 13 summarizes the three relations. As already remarked in Figure 10, we do not observe much difference in terms of objective distance among the tree sets, while we notice an increasing solution distance for increasing tree distance.

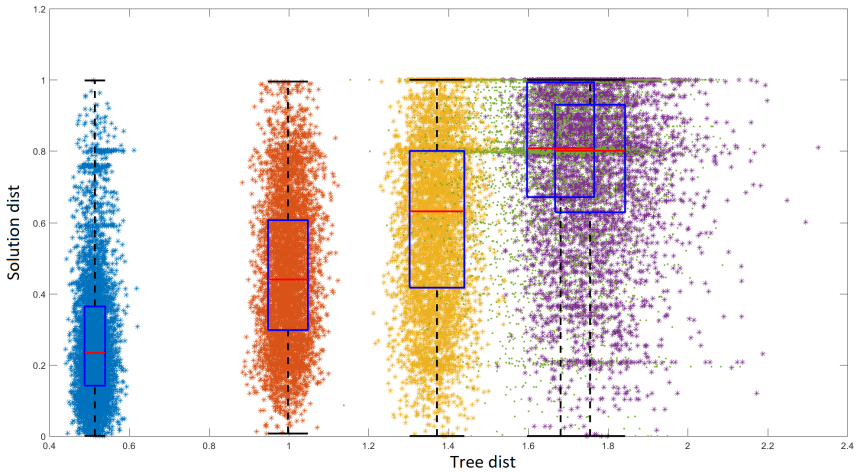

Fig. 11. Solution distance in relation with the tree distance for the expected wealth – AV@R minimization model and corresponding box-plot for each tree set.

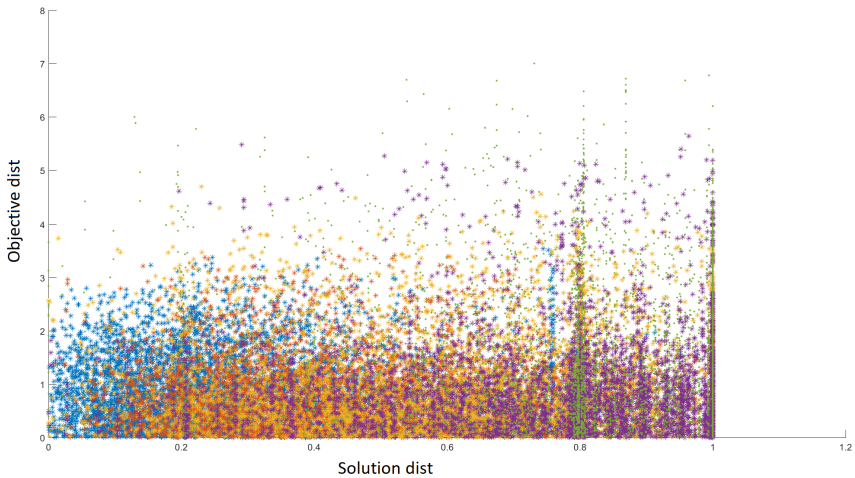

Fig. 12. Objective distance in relation with the solution distance for the expected wealth – AV@R minimization model.

In Table 1 we report the statistics extracted from the box-plots of all the analyzed cases. Thanks to this empirical study, it is possible to confirm that, on average, the multivariate multistage nested distance between the trees generally comoves with the objective distance and with the solution distance.

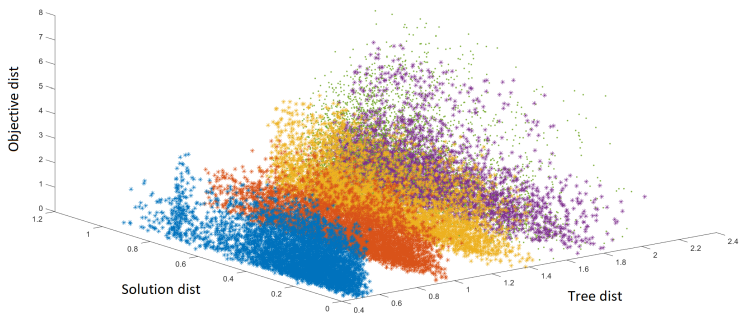

Fig. 13. Relation between objective distance, solution distance and tree distance for the expected wealth – AV@R minimization model.

6. LIPSCHITZ CONSTANT LOWER BOUND

As proved in [11], there exists a Lipschitz constant that multiplied by the tree nested distance produces a bound for the objective distance. Empirically we can compute a lower bound $\underline{L}$ for the true Lipschitz constant L as

$$\underline{L} = \max_{p,q} \frac{d(O_{\mathcal{T}^p}, O_{\mathcal{T}^q})}{d(\mathcal{T}^p, \mathcal{T}^q)} \tag{13}$$

for each tree set and for each model. The estimated values of $\underline{L}$ are reported in Table 2. However, we empirically show that, for each tree set, the objective distances are not concentrated close to the point corresponding to the solution of (13) and then the lower bound $\underline{L}$ of the Lipschitz constant does not produce a strict bound for the objective distance.

7. CONCLUSION

To summarize, it has been empirically proven that there exists a positive relation between the multistage multivariate nested distance of the stochastic trees and the solution distance, as well as a positive relation between the multistage multivariate nested distance of the stochastic trees and the objective distance. Moreover, we have shown that the Lipschitz constant that bounds the objective distance is not a strict bound. Further research could use the multivariate multistage nested distance to investigate the distance between stochastic trees with a highly different number of nodes and to theoretically define and empirically study a measure between stochastic trees with a different number of stages.

			AV@R		Expected value		Expected-AV@R	
Distances between:		tree	obj	sol	obj	sol	obj	sol
$\mathcal{T}_{GBM,3}$	avg	0.51	1.77	0.28	0.60	0.00	0.95	0.27
	std	0.02	1.27	0.17	0.44	0.00	0.69	0.19
	min	0.44	0.00	0.00	0.00	0.00	0.00	0.00
	max	0.62	6.80	1.00	2.38	0.01	3.54	1.00
$\mathcal{T}_{GBM,2}$	avg	1.00	2.29	0.47	1.09	0.00	0.75	0.46
	std	0.04	1.66	0.22	0.79	0.00	0.63	0.21
	min	0.88	0.00	0.00	0.00	0.00	0.00	0.01
	max	1.12	9.11	1.00	4.91	0.01	3.54	1.00
$\mathcal{T}_{GBM,1}$	avg	1.37	2.65	0.56	1.45	0.10	1.00	0.60
	std	0.05	2.11	0.29	1.08	0.10	0.88	0.24
	min	1.21	0.00	0.00	0.00	0.00	0.00	0.00
	max	1.58	13.03	1.00	6.09	0.40	4.70	1.00
$\mathcal{T}_{GBM,0}$	avg	1.76	3.16	0.80	3.00	0.85	0.94	0.75
	std	0.10	2.56	0.22	2.32	0.28	0.90	0.22
	min	1.49	0.00	0.00	0.00	0.00	0.00	0.00
	max	2.33	18.06	1.00	13.82	1.00	5.64	1.00
$\mathcal{T}_{HIST}$	avg	1.68	3.94	0.81	2.88	0.87	1.53	0.78
	std	0.14	2.87	0.23	2.22	0.27	1.28	0.23
	min	1.14	0.00	0.00	0.00	0.00	0.00	0.00
	max	2.16	17.17	1.00	12.58	1.00	7.00	1.00

Tab. 1. Statistics of the computed distances for the different tree sets and the different portfolio models: average (avg), standard deviation (std), minimum (min) and maximum (max).

	AV@R	Expected value	Expected-AV@R
$\mathcal{T}_{GBM,3}$	12.98	4.73	6.88
$\mathcal{T}_{GBM,2}$	9.20	5.26	3.47
$\mathcal{T}_{GBM,1}$	9.69	4.45	3.60
$\mathcal{T}_{GBM,0}$	9.25	6.59	3.12
$\mathcal{T}_{HIST}$	9.09	7.82	3.93

Tab. 2. Lipschitz constant lower bound for the different tree sets and the different portfolio models.

ACKNOWLEDGEMENT

This work was supported by the Czech Science Foundation project GAČR No. 18-01781Y.

(Received November 24, 2017)

REFERENCES

[1] J. R. Birge and F. Louveaux: Introduction to Stochastic Programming. Springer Science and Business Media, 2011.

[2] G. Consigli, V. Moriggia, E. Benincasa, G. Landoni, F. Petronio, S. Vitali, M. di Tria, M. Skoric, and A. Uristani: Optimal multistage defined-benefit pension fund management. In: Recent Advances in Commmodity and Financial Modeling: Quantitative methods in Banking, Finance, Insurance, Energy and Commodity markets (G. Consigli, S. Stefani, and G. Zambruno eds.), Springer's International Series in Operations Research and Management Science, 2017. DOI:10.1007/978-3-319-61320-8_13

[3] J. Dupačová, J. Hurt, and J. Štěpán: Stochastic Modeling in Economics and Finance. Applied Optimization, Springer, 2002. DOI:10.1007/b101992

[4] S. Kilianová and G. C. Pflug: Optimal pension fund management under multi-period risk minimization. Ann. Oper. Res. *166* (2009), 1, 261–270. DOI:10.1007/b101992

[5] M. Kopa and B. Petrová: Multistage risk premiums in portfolio optimization. Kybernetika *53* (2017), 6, 992–1011. DOI:10.14736/kyb-2017-6-0992

[6] M. Kopa, V. Moriggia, and S. Vitali: Individual optimal pension allocation under stochastic dominance constraints. Ann. Oper. Res. *260* (2018), 1,2, 255–291. DOI:10.1007/s10479-016-2387-x

[7] R. M. Kovacevic and A. Pichler: Tree approximation for discrete time stochastic processes: a process distance approach. Ann. Oper. Res. *235* (2015), 1, 395–421. DOI:10.1007/s10479-015-1994-2

[8] F. Maggioni and G. C. Pflug: Bounds and approximations for multistage stochastic programs. SIAM J. Optim. *26* (2016), 1, 831–855. DOI:10.1137/140971889

[9] F. Maggioni, E. Allevi, and M. Bertocchi: Bounds in multistage linear stochastic programming. J. Optim. Theory Appl. *163* (2014), 1, 200–229. DOI:10.1007/s10957-013-0450-1

[10] F. Maggioni, E. Allevi, and M. Bertocchi: Monotonic bounds in multistage mixed-integer liner stochastic programming. Comput. Management Sci. *13* (2016), 3, 423–457. DOI:10.1007/s10287-016-0254-5

[11] G. C. Pflug and A. Pichler: A distance for multistage stochastic optimization models. SIAM J. Optim. *22* (2012), 1, 1–23. DOI:10.1137/110825054

[12] G. C. Pflug and A. Pichler: Multistage Stochastic Optimization. Springer, 2014. DOI:10.1007/978-3-319-08843-3

[13] G. C. Pflug and A. Pichler: Convergence of the smoothed empirical process in nested distance. Humboldt-Universität zu Berlin, Mathematisch-Naturwissenschaftliche Fakultät II, Institut fűr Mathematik (J. L. Higle, W. Römisch, and S. Surrajeet, eds.), 2015.

[14] G. C. Pflug and A. Pichler: From empirical observations to tree models for stochastic optimization: Convergence properties. SIAM J. Optim. *26* (2016), 3, 1715–1740. DOI:10.1137/15m1043376

[15] W. B. Powell: Clearing the jungle of stochastic optimization. Informs TutORials, 2014. DOI:10.1287/educ.2014.0128

[16] T. R. Rockafellar and S. Uryasev: Optimization of conditional value-at-risk. J. Risk *2* (2000), 21–42. DOI:10.21314/jor.2000.038

[17] A. Shapiro, D. Dentcheva, and A. Ruszczyński: Lectures on stochastic programing. Modeling and Theory. SIAM Math. Programm. Soc. 2009.

[18] A. V. Timonina: Multi-stage stochastic optimization: the distance between stochastic scenario processes. Computat. Management Sci. *12* (2015), 1, 171–195. DOI:10.1007/s10287-013-0185-3

[19] S. Vitali, V. Moriggia, and M. Kopa: Optimal pension fund composition for an Italian private pension plan sponsor. Comput. Management Sci. *14* (2017), 1, 135–160. DOI:10.1007/s10287-016-0263-4

Sebastiano Vitali, Charles University in Prague, Faculty of Mathematics and Physics, Department of Probability and Mathematical Statistics, Sokolovská 83, 186 75 Praha 8. Czech Republic.

e-mail: vitali@karlin.mff.cuni.cz